Quantifying the Natural Radioactivity and Assessing the Radiation Risks in Different Rock Types at Wadi Nassib Area

Journal of Physics: Conference Series **2830** (2024) 012025 doi:10.1088/1742-6596/2830/1/012025

Quantifying the Natural Radioactivity and Assessing the Radiation Risks in Different Rock Types at Wadi Nassib Area

Hesham A. Yousef [1], M. A. Ibrahim[1], T. I. Elsobky[1,2], N. A. Kawady[2], A. Alshami [2], M. G. El Feky [2]
[1] Physics Department, Faculty of Science, Suez University, P.O. Box: 43221, Suez, Egypt
[2] Nuclear Materials Authority, El-Maadi, P.O. Box 530, Cairo, Egypt.

tamer.elsobky6@gmail.com

Abstract. Wadi Nassib, Egypt, has significantly higher natural radiation levels compared to global averages, particularly in uranium, thorium, radium, and potassium. This raises concerns for resident health due to potential radiation exposure. The study suggests these elements may have different origins and emphasizes the need for monitoring and managing such elevated natural radioactivity.

1. Introduction

There are two types of radiation that affect humans: external and internal. External radiation comes from outside the body and targets it directly, while internal radiation enters the body through ingestion or inhalation, potentially harming internal tissues. External sources of radiation from Earth's crust include gamma rays, and internal exposure comes from radon, thoron, their decay products, as well as food, water, and other environmental sources. Radioactive elements found in soil and building materials in small quantities result in different levels of radiation exposure. Volcanic rocks, like granite, have a higher radiation emission rate than sedimentary rocks, such as shale [1]. The main sources of gamma radiation exposure are the decay of ^{238}U and ^{232}Th, as well as naturally occurring ^{40}K [2]. Extended contact with radioactive substances and breathing in radioactive particles pose serious health hazards. Some of these conditions are acute leukaemia, anaemia, and necrosis. Exposure to radium can result in anaemia, cataracts, and different forms of cancer. Likewise, exposure to thorium can lead to lung, pancreas, liver, bone, and kidney cancers, as well as leukemia [3].

Southwest Sinai's Paleozoic rocks were divided into three units: Lower Sandstone, Carboniferous Limestone, and Upper Sandstone Series. The Lower Sandstone Series is made up of three formations in sequential order; Sarabit El Khadim, Abu Hamata, and Adadia Formations. Fossil imprints confirmed that the Lower Sandstone Series dates back to the Cambro-Ordovician period. The Um Bogma Formation is the present name for the Carboniferous Limestone Series. The Formation is made up of three layers in the following order: siltstone, dolostone, and claystone at the bottom; marl and dolostone in the middle; and dolostone, siltstone, and claystone at the top. The Upper Sandstone Series is subdivided into three formations in order from oldest to youngest: El Hashash, Magharet El Maiah, and Abu Zarab. Lower Carboniferous sediments are notably well developed in the southwestern regions.

The Paleozoic stratum is important economically because it contains valuable minerals and ore deposits such as uranium (U), manganese (Mn), ferromanganese (Fe-Mn), and copper (Cu). This research centers on the Um Bogma Formation, which contains the most important uranium reserves in its sedimentary strata. The formation is located below (conformably underlies) the EL Hashash Formation and is supported by older, uneven layers (unconformably overlies) of the Adadia Formation. Weissbord, 1969 was the first to create the name Um Bogma Formation for the carbonate rocks in the Um Bogma area, identifying it as the reference location (type locality). This work mainly aims to discuss the factors that control the distribution of radionuclides and detect the hazards indices in Wadi Nassib area.

2. Geological setting

Um Bogma Formation is considered one of the most important sediments in south west Sinai. The uranium bearing sediments are mainly confined and associated with Um Bogma Formation. These sediments were affected by several faults, comprising normal, reverse, strike-slip and, step faults. Allouga region is located at the western side of Wadi Naassib faults. Um Bogma Formation is a collection of sedimentary rocks including gibbsite-bearing sediments, shale, ferruginous siltstone, marl, dolostone, clay, and iron-manganese (Fe-Mn) **ore** (Figure 1) [4]. The studied area is 35 kilometers east of Abu Zenima city. The present study focuses on dolostone. The uranium-bearing facies contain various uranium minerals, including oxides, silicates, uranyl-oxyhydroxides, phosphates, arsenates, vanadates, molybdates, carbonates, and sulfate complexes.

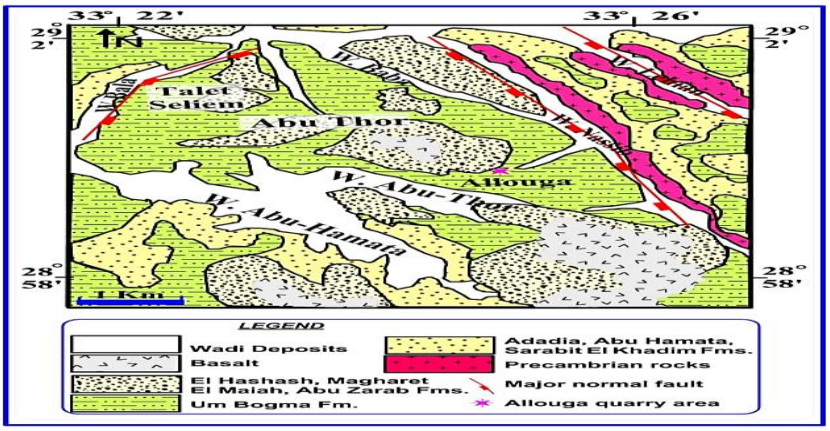

Figure 1. Geologic map of Allouga showing different rock units.

3. Sample preparation

Prior to radiation measurements, twenty-four rock samples from Wadi Nasseib region were crushed to a grain size of 250 µm. The compressed samples were subsequently enclosed using heavy vinyl tape to avoid the release of radon gas from PVC cylindrical containers (9.5 cm in diameter, 3 cm in height) and prevent gas leakage. Afterwards, the containers were kept for at least four weeks [5]. A Bicron 3" x 3" NaI (Tl) detector was placed inside a shielding system with multiple layers for gamma-ray spectroscopy. The most internal layer included a copper cylinder with a thickness of 0.6 cm, followed by a lead shield that was 5 cm thick. Another lead covering was given to increase protection. The detector was linked to a Nuclear Enterprises NE-4658 primary shaping amplifier and a Tennelec TC 952 high voltage power source. Data acquisition was performed using an 8k multichannel analyser known as Nuclease PCA-8000. Concentrations of ^{238}U (found from the 92.5 keV γ-ray of ^{234}Th), ^{232}Th (detected with the 238.6 keV γ-ray of ^{212}Pb), ^{226}Ra (calculated using the 352.0 keV γ-ray of ^{214}Pb), and ^{40}K (examined with the 1460 keV γ-ray) were determined **[5]**.

4. Radiological hazards assessment

Radiation hazard assessments leverage specialized equations based on measured radioactive elements in Bq kg^{-1} to determine potential radiation risks to the general public, aiding in preventative measures and safeguarding well-being.

4.1 Radium equivalent (Ra_{eq})

The radiation risk from environmental materials like soil requires considering different radioactive elements. Ra_{eq}, developed by Beretka and Mathew, simplifies this by combining their effects into a single, easy-to-interpret value, aiding in risk assessment and regulatory decision-making [2, 6].

$$\boldsymbol{Ra_{eq} = A_{Ra} + 1.43\ A_{Th} + 0.077\ A_K} \quad \textbf{(1)}$$

where A_{Ra}, A_{Th}, and A_K are the specific activities of ^{226}Ra, ^{232}Th, and ^{40}K, respectively, in Bq kg^{-1}. The accepted value of Ra_{eq} is below 369 Bq kg^{-1} [7].

4.2 Estimation of the absorbed dose rate (DR) and annual effective dose rate (AEDR)

Based on the guidelines set by UNSCEAR 1993 **[8]** the-D_R in outdoor air (nGyh^{-1}) is estimates basically from three γ-ray emitters, which are naturally occurring radionuclides: ^{226}Ra, ^{232}Th, and ^{40}K uniformly distributed at one metre above the ground surface, whereas other minor contributions from radionuclides are neglected. Therefore, D_R can be calculated by [2];

$$\boldsymbol{D_R = 0.462A_{Ra} + 0.604A_{Th} + 0.0417A_K} \quad \textbf{(2)}$$

where A_{Ra}, A_{Th} and A_K are the activity concentrations of ^{226}Ra, ^{232} Th, and ^{40}K, respectively, in Bq kg^{-1}.

The AEDR outdoor estimated by

$$\textbf{AEDR}\left(\boldsymbol{mSvy^{-1}}\right) = \boldsymbol{D_R \times F \times DCF \times 8760 \times 10^{-6}} \quad \textbf{(3)}$$

where F is related to the values of the occupancy factor (0.8 for indoors and 0.2 for outdoors). DCF is stands for the dose conversion factor (0.7 $SvGy^{-1}$), the number of hours in a year (8760 h); the average annual external effective dose from terrestrial radionuclides is 0.46 $mSvy^{-1}$ **[9]**.

*4.3 External hazard index (H_{ex}) **and** Internal hazard index (H_{in})*

Beretka and Mathew **[9]** proposed hazard indices to manage radiation exposure from building materials**.** These indices translate the Ra_{eq} value, which reflects the combined potential radiation risk from naturally occurring radionuclides, into two distinct components: H_{ex} and H_{in} indices**.** Keeping both indices below 1 ensures that the total radiation dose from the material stays within the permissible annual limit of 1 mSv [2].

$$\mathbf{H_{in}} = \frac{\mathbf{A_{Ra}}}{\mathbf{370}} + \frac{\mathbf{A_{Th}}}{\mathbf{259}} + \frac{\mathbf{A_K}}{\mathbf{4810}} \quad \textbf{(4)}$$

$$\boldsymbol{H_{ex}} = \frac{\boldsymbol{A_{Ra}}}{\mathbf{185}} + \frac{\boldsymbol{A_{Th}}}{\mathbf{259}} + \frac{\boldsymbol{A_K}}{\mathbf{4810}} \quad \textbf{(5)}$$

where A_{Ra}, A_{Th}, and A_K represent the activity concentration of ^{226}Ra,^{232}Th and ^{40}K, respectively.

4.4 γ-radiation level index Iγ

The I_γ index is a screening tool to identify materials that may pose health concerns due to their radiation levels. The acceptable I_γ value should be ≤1. I_γ can be calculated using the following formula **[10]**

$$\mathbf{I_\gamma} = \frac{\mathbf{A_{Ra}}}{\mathbf{150}} + \frac{\mathbf{A_{Th}}}{\mathbf{100}} + \frac{\mathbf{A_K}}{\mathbf{1500}} \leq \mathbf{1} \quad \textbf{(6)}$$

where A_{Ra}, A_{Th}, and A_K are the specific activities of ^{226}Ra, ^{232}Th, and ^{40}K, respectively, in Bq kg^{-1}.

5. Results

Twenty-four samples collected from Wadi Nassib area were examined for naturally-occurring radioactive elements such as ^{238}U, ^{232}Th, ^{226}Ra, and ^{40}K. **Tables 1 and 2** display the measured activities and hazard indices, while Table 3 outlines key statistical parameters for these elements and indices. The measured activity concentrations of ^{238}U, ^{232}Th, ^{226}Ra, and ^{40}K in the samples exhibited significant differences from global averages. On average, the concentrations were 17820.65 ± 56318.28 Bq kg^{-1}, 51.63 ± 50.82 Bq kg^{-1}, 5341.85 Bq kg^{-1} ± 4534.20 Bq kg^{-1}, and 473.67 ± 445.80 Bq kg^{-1}, respectively. These values are considerably higher than the global averages reported in the UNSCEAR 2008 report [12], which indicated that average concentrations of these natural radionuclides in soils typically remain low. While acknowledges a significant spread, with documented levels reaching 1,000 Bq kg^{-1} for ^{238}U, 360 Bq kg^{-1} for ^{232}Th, and 3200 Bq Kg^{-1} for ^{40}K, the observed values in this study far exceed even these upper limits. Table 3 summarizes the descriptive statistics the measured activity concentrations for ^{238}U, ^{232}Th, ^{226}Ra, and ^{40}K in the Wadi Nassib area samples. To visually explore the distribution patterns of these natural radionuclides, histograms were generated for each element (Figure 3). These histograms reveal details about the frequency distribution of activity concentrations, to identify potential trends, outliers, and deviations from normality.

Normality tests revealed a non-normal distribution for ^{238}U, as indicated by the Shapiro-Wilk test of normality ($p = 0.0196, < 0.05$). This suggests a departure from normality, while ^{232}Th, ^{226}Ra, and ^{40}K appear normally distributed based on the same test. Also, Table 3 shows that only ^{232}Th has an approximately symmetrical distribution and exhibits a tendency towards lower values. The remaining elements (^{238}U, ^{226}Ra, and ^{40}K) exhibit positive skewness, indicating right-skewed distributions with a bias towards higher values. These findings suggest a potential migration of these skewed elements towards Allouga area, leading to their elevated concentrations. This interpretation may be further supported by evidence demonstrating that thorium exhibits a greater resistance to leaching compared to uranium.

Table 1. Radionuclide's concentration.

Sample	^{238}U (ppm)	^{232}Th (ppm)	^{226}Ra (ppm)	^{40}K %
Alg 01	67.59	9.71	9.68	0.89
Alg 02	92.47	9.77	68.01	1.37
Alg 03	46.78	28.42	36.04	2.33
Alg 04	7.45	8.57	13.69	1.33
Alg 05	478.97	7.53	127.25	3.61
Alg 06	2186	1.5	892.29	0.1
Alg 07	121.54	7.16	63.2	1.06
Alg 08	844.03	1.5	1438.03	2.36
Alg 09	1856.99	1.5	601.63	1.7
Alg 10	2344.09	1.5	1268.42	5.4
Alg 11	328.37	16.88	696.61	0.1
Alg 12	348.12	25.7	689	0.1
Alg 13	580.88	1.5	1264.19	4.03
Alg 14	685.41	1.5	534.93	3.02
Alg 15	1	32.15	342.55	0.25
Alg 16	1	35.12	309.68	0.74
Alg 17	1	33.59	313.03	0.59
Alg 18	1	24.57	343.41	1.26
Alg 19	686.31	1.5	524.13	1.56
Alg 20	22615	1.5	556.94	0.1
Alg 21	298.1	30.2	678.06	0.1
Alg 22	252.29	1.5	357.01	1.53
Alg 23	108.84	1.5	202.7	2.69
Alg 24	677.99	22.48	219.46	0.1

Table 2. calculations of hazard indices under study.

Sample	Ra_{eq}	D_R (nGy h^{-1})	AED ($mSvy^{-1}$)	H_{in}	H_{ex}	I_γ
Alg 01	184.99	84.95	0.10	4.72	2.47	1.29
Alg 02	844.37	390.49	0.48	6.41	3.33	5.71
Alg 03	620.39	284.58	0.35	3.72	2.16	4.30
Alg 04	233.52	108.48	0.13	0.72	0.47	1.64
Alg 05	1542.98	718.06	0.88	32.33	16.34	10.47
Alg 06	9915.49	4580.81	5.62	145.96	73.00	66.11
Alg 07	768.43	355.41	0.44	8.29	4.24	5.19
Alg 08	16027.68	7408.97	9.09	56.52	28.35	106.97
Alg 09	6727.73	3111.13	3.82	124.10	62.12	44.94
Alg 10	14218.27	6578.85	8.07	156.86	78.62	95.05
Alg 11	7832.30	3614.85	4.43	22.19	11.23	52.25
Alg 12	7798.78	3597.35	4.41	23.65	12.03	52.05
Alg 13	14138.30	6539.28	8.02	39.06	19.67	94.45
Alg 14	6019.17	2786.31	3.42	45.98	23.10	40.28
Alg 15	3994.07	1838.38	2.25	0.58	0.55	26.70
Alg 16	3658.18	1683.46	2.06	0.66	0.63	24.49
Alg 17	3682.91	1694.95	2.08	0.63	0.60	24.64
Alg 18	3984.16	1837.48	2.25	0.53	0.50	26.67
Alg 19	5864.11	2711.86	3.33	45.94	23.03	39.17
Alg 20	6193.11	2861.07	3.51	1509.73	754.88	41.30
Alg 21	7703.35	3552.23	4.36	20.38	10.43	51.42
Alg 22	4008.35	1854.45	2.27	16.97	8.54	26.80
Alg 23	2323.47	1078.26	1.32	7.46	3.83	15.62
Alg 24	2568.29	1181.59	1.45	45.62	22.99	17.17

Table 3. Statistical analysis for the measured natural radionuclides activity levels of ^{238}U, ^{232}Th, ^{226}Ra, and ^{40}K in Wadi Nassib area samples.

Column	Mean	Std Dev	Std. Error	C.I. of Mean	Range	Skewness	Kurtosis
A ^{238}U ($Bqkg^{-1}$)	17820.66	56318.28	11495.92	23781.12	279282.90	4.73	22.81
A ^{232}Th ($Bqkg^{-1}$)	51.653	50.824	10.374	21.46	135.83	0.63	-1.30
A ^{226}Ra ($Bqkg^{-1}$)	5341.85	4534.20	925.54	1914.63	15854.69	0.98	0.33
A ^{40}k ($Bqkg^{-1}$)	473.67	445.79	90.997	188.24	1658.90	1.14	1.00
Ra_{eq} ($Bqkg^{-1}$)	5452.18	4523.16	923.29	1909.96	15842.68	0.98	0.34
D_R ($nGyh^{-1}$)	2518.88	2091.49	426.92	883.16	7324.02	0.98	0.35
AED ($mSvy^{-1}$)	3.09	2.565	0.52	1.08	8.98	0.98	0.35
H_{in}	96.63	304.36	62.13	128.52	1509.20	4.73	22.81
H_{ex}	48.46	152.15	31.06	64.25	754.41	4.73	22.81
I_γ	36.45	30.17	6.16	12.74	105.67	0.98	0.35

The previous result was also indicated by eTh/eU with both eU and eTh correlation, where the eTh/eU ratio is smaller than the known ratios from approximately 4:1 to 10:1 or even higher in certain cases.[11] (Figures 2a, 2b). eTh-K-eTh-U binary relations exhibit weak to very weak correlation, suggesting the role of alteration processes in the mobility of these elements, which was induced by their ratios (eTh/eU-eTh/K). All samples plot in the fixed zone due to the prevailing reduction conditions during uranium precipitation (Figure 2c). The U-K/U (Figure 2d) relationship shows potassium that are lower than the international levels as a result of uranium enrichment.

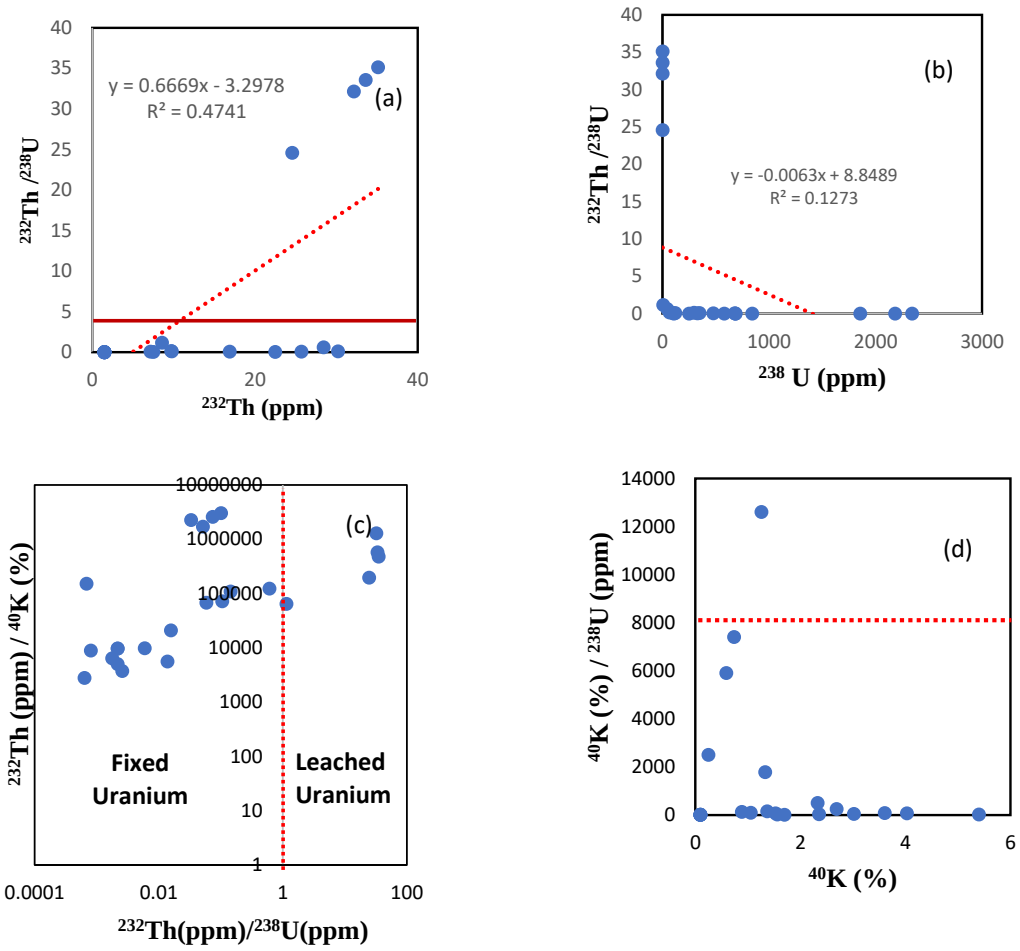

Figure 2. Natural radioactive elements relations in the studied samples.

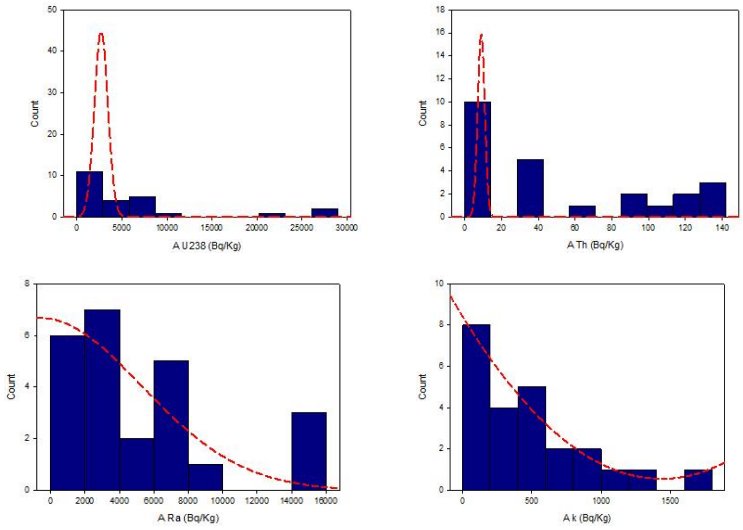

Figure 3. Histogram of radionuclides.

Statistical analysis suggests (Figure 3) a potential shared origin for ^{226}Ra and ^{40}K, as their data aligns with a normal distribution. This finding implies that these elements might have stemmed from the same population or experienced similar processes leading to their current distribution. In contrast, the ^{238}U and ^{232}Th data significantly deviate from normality, indicating a different underlying distribution. This difference suggests these elements might have undergone distinct processes or originated from separate sources compared to ^{226}Ra and ^{40}K. An intriguing pattern emerges from the correlations observed between naturally occurring radioactive elements (Table 4). Notably, ^{238}U exhibits a weak negative correlation with both ^{232}Th and ^{40}K (-0.264 and -0.158, respectively), implying that higher concentrations of ^{238}U tend to coincide with lower ^{232}Th and ^{40}K concentrations. this clarifying uranium mobilization in conditions different from thorium due to oxidation processes, which is related to the changes in the physic-chemical conditions. Conversely, ^{226}Ra demonstrates a weak positive correlation with ^{238}U (0.132). This suggests disequilibrium in the uranium series in the studied area.

On the other hand, ^{232}Th exhibits a negative correlation with both ^{226}Ra (-0.315) and ^{40}K (-0.490), indicating a moderate decrease in their concentrations as ^{232}Th increases. This suggests potential processes where the decay of ^{232}Th leads to the depletion of both ^{226}Ra and ^{40}K. Interestingly, ^{226}Ra and ^{40}K show a weak positive correlation (0.322), implying a possible slight rise in ^{40}K alongside increasing ^{226}Ra. This finding warrants further investigation to explore potential underlying mechanisms and exceptions to this trend.

Table 4. Pearson correlations between Natural radioactive elements.

Variables	**^{238}U (Bq kg^{-1})**	**^{232}Th (Bq kg^{-1})**	**^{226}Ra (Bq kg^{-1})**	**^{40}K (Bq kg^{-1})**
^{238}U (Bq kg^{-1})	1	-0.264	0.132	-0.158
^{232}Th (Bq kg^{-1})	- 0.264	1	-0.315	-0.490
^{226}Ra (Bq kg^{-1})	0.132	-0.315	1	0.332
^{40}K (Bq kg^{-1})	-0.158	-0.490	0.332	1

5.1Hazard indices

Analysis of Ra_{eq} **(Tables 2, 3)** revealed a mean value of 5452 ± 4523.16 Bq kg^{-1}, significantly exceeding the reported limit of 370 Bq kg^{-1} **[12]**. These elevated Ra_{eq} values suggest a profound influence of ^{226}Ra by 98% to total Ra_{eq} in the studied area. This observation warrants further investigation to explore the specific mechanisms and contributing factors responsible for such high levels.

5.2 External and internal hazard indices

H_{ex} values ranged from 0.469 to a staggering 754.882 Bq kg^{-1}, while H_{in} values spanned from 0.532 to an even more alarming 1509.734 Bq kg^{-1}. Notably, the average values for both indices were significantly elevated, reaching 48.462 and 96.626 Bq kg^{-1}, respectively [2]. The calculated D_R values (Tables 2, 3) exhibit that the mean value is 2518.884 nGyh^{-1} and ranged between 84.951 and 7408.969, which is more than the reported limit of 59 nGyh^{-1} [13].

The average of ADER from terrestrial radionuclides is 0.46 mSv y^{-1} [14]. This study revealed that AED values (Tables 2, 3) ranged from low value of 0.104 to high value of 9.086 mSvy^{-1} with an average of 3.089 mSvy^{-1}**.** Notably, the maximum observed AED value significantly exceeded the recommended upper limit. While the gamma index (I_γ) shouldn't exceed 1 µRhr^{-1} [11]. This study revealed that I_γ values (Tables 2, 3) ranged from 1.294 to 106.967 µRh r^{-1}, with an average of 36.445 µRhr^{-1}. Notably, the maximum observed I_γ value significantly exceeded the recommended upper limit, so unsuitable for use as building materials [15]. Principal Component Analysis (PCA) explores the relationships between the identified components. It utilizes the components' correlation matrix to pinpoint the main factors influencing the data and the proportion of variance explained by each component (as illustrated in Figure 4).

The analysis reveals a weak positive association of ^{226}Ra, ^{238}U, and a weak value for ^{40}K activity concentrations with the first principal component (PC1), which explains a significant 53.81% of the total variance in the data. The second component (PC2) explains 29.96% of the variance and is associated with ^{238}U, and weak negative correlations to the rest activity concentrations. This suggests that ^{226}Ra and ^{238}U are the primary sources of gamma radiation in the analysed samples. Notably, ^{40}K and ^{232}Th are also likely to contribute but are not directly highlighted in the PCA due to their correlation with either ^{226}Ra or ^{238}U.

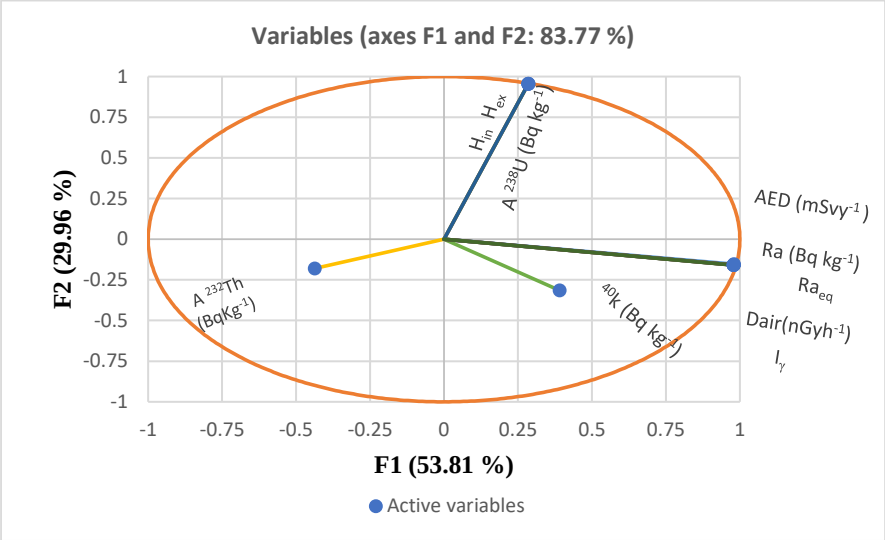

Figure 4. PCA.

References

[1] Vinay Kumar Reddy K, Srinivas Reddy G, Muralikrishna P, Shravan Kumar Reddy S and Sreenivasa Reddy B 2023 Natural background outdoor gamma radiation levels and mapping of associated risk in Siddipet district of Telanagana State, India Nuclear and Particle Physics Proceedings.

[2] Nations Scientific Committee on the Effects of Atomic Radiation U SOURCES AND EFFECTS OF IONIZING RADIATION United Nations Scientific Committee On The Effects Of Atomic Radiation UNSCEAR 2000 Report To The General Assembly, With Scientific Annexes Volume I: Sources United Nations.

[3] Chandrasekaran A, Ravisankar R, Senthilkumar G, Thillaivelavan K, Dhinakaran B, Vijayagopal P, Bramha S N and Venkatraman B 2014 Spatial distribution and lifetime cancer risk due to gamma radioactivity in Yelagiri Hills, Tamilnadu, India Egyptian Journal of Basic and Applied Sciences 1 38–48.

[4] A Alshami A S 2018 U-Minerals And Ree Distribution, Paragenesis And Provenance, Um Bogma F O Rmation Southwestern Sinai, Egypt 31–55.

[5] Tawfic A F, Omar A, Abed N S and Tantawy H R 2021 Investigation of Natural Radioactivity in Wadi El Reddah Stream Sediments and Its Radiological Implications Radiochemistry 63 243–50.

[6] Beretka J and Mathew P J 1985 Natural Radioactivity of Australian Building Materials, Industrial Wastes and By-products Health Phys 48 87–95.

[7] El-Afandy A H, El-Feky M G, Taha S H, El Minyawi S M, Sallam H A, Tawfic A F, Omar A and El-Samrah M G 2022 Radioactivity and Environmental Impacts of Granites from Um Ara, Southeastern Desert, Egypt Journal of Physics: Conference Series vol 2305 (Institute of Physics).

[8] Nations Scientific Committee on the Effects of Atomic Radiation U SOURCES AND EFFECTS OF IONIZING RADIATION United Nations Scientific Committee on the Effects of Atomic Radiation UNSCEAR 1993 Report to the General Assembly, with Scientific Annexes UNITED NATIONS.
[9] Shabaka A N, Omar A, El-Mongy S A and Tawfic A F 2022 Analysis of natural radionuclides and 137Cs using HPGe spectrometer and radiological hazards assessment for Al-Nigella site, Egypt Int J Environ Anal Chem 102 575–88.
[10] Agbalagba E O, Avwiri G O and Chad-Umoreh Y E 2012 γ-Spectroscopy measurement of natural radioactivity and assessment of radiation hazard indices in soil samples from oil fields environment of Delta State, Nigeria J Environ Radioact 109 64–70.
[11] El-Kammar A M, El-Feky M G, Hassan; Abu Zied T and Othman D A 2018 Radioactivity And Environmental Impacts Of Some Carboniferous And Cretaceous Kaolin Deposits In Southwestern-Sinai, EGYPT.
[12] United Nations. Scientific Committee on the Effects of Atomic Radiation. 2010 Sources and effects of ionizing radiation: United Nations Scientific Committee on the Effects of Atomic Radiation: UNSCEAR 2008 report to the General Assembly, with scientific annexes. (United Nations).
[13] Mbonu C C and Ben U C 2021 Assessment of radiation hazard indices due to natural radioactivity in soil samples from Orlu, Imo State, Nigeria Heliyon 7.
[14] Nations Scientific Committee On The Effects Of Atomic Radiation U Sources And Effects Of Ionizing Radiation United Nations Scientific Committee on The Effects of Atomic Radiation Unscear 1993 Report To The General Assembly, With Scientific Annexes United Nations.
[15] Yalcin F, Ilbeyli N, Demirbilek M, Yalcin M G, Gunes A, Kaygusuz A And Ozmen S F 2020 Estimation Of Natural Radionuclides' Concentration Of The Plutonic Rocks In The Sakarya Zone, Turkey Using Multivariate Statistical Methods Symmetry (Basel) 12 1–18.